

TOPOGRAPHIC MAPPING OF TITAN: LATEST RESULTS. R.L. Kirk¹, E. Howington-Kraus¹, B. Redding¹, P.S. Callahan², A.G. Hayes³, A. Le Gall⁴, R.M.C. Lopes², R.D. Lorenz⁵, A. Lucas⁶, K.L. Mitchell², C.D. Neish⁵, O. Aharonson⁶, J. Radebaugh⁷, B.W. Stiles², E.R. Stofan⁸, S.D. Wall², C.A. Wood⁹, ¹Astrogeology Science Center, USGS, 2255 N. Gemini Dr., Flagstaff AZ 86001 (rkirk@usgs.gov), ²Jet Propulsion Laboratory, Pasadena, CA 91109, ³Univ. of California, Berkeley, CA 94720, ⁴LATMOS-UVSQ, Paris, France, ⁵Johns Hopkins Univ. Applied Physics Lab, Laurel, MD 20723, ⁶Caltech, Pasadena, CA 91125, ⁷Brigham Young Univ., Provo, UT 84602, ⁸Proxemy Research, Gaithersburg, MD 20882, ⁹Wheeling Jesuit Univ., Wheeling, WV 26003.

Introduction: This abstract is one of a series of reports on our qualitative [1] and quantitative [2–6] assessments of the topography of Saturn’s satellite Titan at resolutions as high as a few kilometres, based on radargrammetric analysis of stereo image pairs from the Cassini RADAR [7]. This instrument uses microwaves with 2.2-cm λ to form synthetic aperture (SAR) images with 350–1400 m resolution, as well as obtaining radiometric, scatterometric, and altimetric data. To date, the instrument has obtained full resolution SAR swaths useful for stereomapping on 33 Titan flybys between Ta and T77. These images form 110 possible stereopairs, covering a combined area greater than 2% of Titan.

Our first digital topographic model (DTM) of Titan [2] was uncontrolled, i.e., terrain coordinates were derived from the spacecraft trajectory as reconstructed by the Cassini mission. Because of the geometry of radar image formation, errors in horizontal position of the DTM are comparable to the trajectory uncertainties, but errors in absolute vertical elevation can be somewhat magnified. Some of the models reported in [3] can be considered semicontrolled; although each DTM was produced by the same process as [2], they were adjusted after the fact by a vertical translation to eliminate on average any offset from the overlapping elevation data based on monopulse “SARTopo” analysis of the images [8]. The SARTopo profiles have been controlled through a global least-squares adjustment that also incorporates altimetry data, yielding the most accurate and consistent description of Titan’s shape and absolute elevations. Other models in [3] were individually controlled by bundle adjustment based on image-to-image tiepoint measurement and ground control points with elevations constrained by SARTopo data. More recently [5], we performed a joint bundle adjustment of all 6 images in the north polar area of lakes and seas, based on 100 tiepoints and 66 ground control points. A total of 14 controlled DTMs of the circumpolar area (and a DTM of Sotra Facula in the southern overlap of two of the same images [4]) were collected from the adjusted images and found to be consistent at a level suggesting that the precision of matching the images is about 1.4 pixel or 250 m, significantly better than the estimate of ~ 2 pixels that we had made *a priori* based on the noise and variable resolution of the SAR images. This matching precision, combined with the geometry of the stereopairs, permitted us to estimate the vertical precision of each DTM. Values in the range from 50 to 300 m were obtained, with better precision for images with opposite or crossing viewing directions and larger errors for same-side stereo.

In this abstract, we report on several geologically interesting DTMs in the mid latitudes, produced after completion of the north polar control network and individually controlled to SARTopo. We also describe work in progress on adding a recent opposite-look image to the north polar network that will improve the precision of elevation measurements around Ligeia Mare, and on the construction of a southern hemisphere control network that will pave the way for the efficient collection of 20 or more new DTMs.

Technical approach: To perform stereo analysis of Cassini SAR data, we use the software package SOCET SET® available from BAE Systems [9]. The USGS in-house cartographic software package ISIS [10] is used to prepare the images and supporting metadata in formats that the commercial software can understand. SOCET SET provides many

useful capabilities, including bundle adjustment (least-squares adjustment of the spacecraft trajectories to improve the alignment of the images and bring the topographic results into agreement with *a priori* data such as SAR topography elevations); creation of DTMs with powerful and highly adjustable image matching algorithms; and manual quality control, editing, or even *ab initio* creation of DTMs. Given the challenging properties of the RADAR images for stereo matching (modest image size, speckle noise, and differences in illumination between the images), the ability to make interactive measurements by using the stereo display is essential. In some cases, DTM results can be densified and refined by automatic matching after manual “seeding” with a sparse set of height measurements, but in other cases automated matching was not successful and our DTMs were obtained wholly by manual measurement.

The functions noted require a “sensor model,” i.e., software that calculates the image pixel that corresponds to a given ground location in latitude, longitude, and elevation, or the reverse. We used the SOCET Developer’s Toolkit (Dev-kit) to implement such a sensor model for the Cassini RADAR. This model emulates the physical process of SAR image formation in a rigorous way, and distinguishes the nominal spacecraft trajectory used in making the SAR images from the improved trajectory that is estimated in the bundle adjustment process [6].

Titan rotation models: An unexpected result [3] was that some stereopairs (T8-T41 and T13-T43) yielded DTMs with geologically unreasonable overall tilts of several tenths of a degree. These tilts could not be eliminated by adjusting the spacecraft trajectories within their precision of < 1 km, so an ad hoc detrending of these DTMs was performed. The spurious tilts were suspected to be a result of the differing models for Titan’s rotation [11] used in processing SAR images from the Ta to T30 flybys and those from T36 onward. This hypothesis was confirmed when we implemented software to convert the Ta-T30 images and trajectory data to the synchronously rotating model used for T36 on, which can be extrapolated over a longer time base. This conversion was done as part of the process of importing RADAR data into SOCET SET, and eliminated the spurious tilts. Work is now underway to reprocess the Ta-T30 data in the rotational system used for the later images. In addition, we are collecting tiepoints between each new image and the earlier ones it overlaps, with the goal of fitting a definitive and physically reasonable rotation model that will apply to the entire Cassini mission 2004–2017 with high accuracy.

Results:

T08-T61—The mystery of the dunes: Early DTMs [3] showed that Titan’s equatorial dune fields [12] are consistently lower than nearby sand-free areas, but did not resolve the morphology of individual dunes. Because these observations were hampered by the large illumination difference between the images used, the T61 image was designed to yield a near-optimal stereopair of the Belet dune fields in conjunction with T08. The two images overlap between 216° – 252° W and 264° – 310° W, with illumination and viewing from the north side in both (for consistent image appearance to facilitate stereomatching) but with differing incidence angles providing modestly strong stereo. A manually extracted DTM of most of the eastern overlap area resolves the individual dunes where they are most widely spaced (~ 3

km) and indicates peak-to-base elevation differences of 100–200 m. Much to our surprise, given that individual dunes appear radar-dark on a brighter substrate both on Titan and on Earth [13], the bright regions consistently appear higher than the dark regions where they can be resolved. We have considered several possible explanations for this conundrum:

1. There was some sort of mixup with the images, so that the topography appears inverted. This is implausible given that the height calculations are based on a rigorous treatment of the image geometry. Furthermore, the model shows the large sand-free inselbergs are consistently higher than the dune fields, consistent with Earth analogs [12] and previous topographic results [3].
2. It is a perceptual illusion caused by the strong image contrast. This contradicted by the fact that we can track numerous features in the bright areas by blink comparison rather than stereo fusion, and their parallax indicates that they are high.
3. These dark streaks are not dunes in the normal sense, but sand trapped in valleys between parallel ridges of bright material. Candidate explanations for the nature of these ridges are yardangs or fossil dunes, which elsewhere on Titan have dunelike morphology but appear radar-bright [14]. A major problem with this idea is that the “inverted” dunes merge continuously into more densely packed dune fields that resemble those covering most of the equatorial sand seas, and even into what appear to be overlapping longitudinal and transverse dunes (near 8.6° S 237.4° W). Unfortunately, these features are too small for their topography to be resolved, which might provide a definitive answer.
4. The elevated bright areas are not interdunes, but areas of the dune crest and flank that are favorably oriented to have a bright quasi-specular reflection, or perhaps they are a combination of bright quasi-specular reflections from the dunes and adjacent interdunes. The main problem with this idea is that much narrower bright flanks on dunes elsewhere have also been attributed to quasi-specular reflection. If there are two distinct morphologies of dunes with bright reflections, the reason is not understood.

Some support for the final idea listed comes from the observation that the bright zones tend to taper to a point where the dunes end (as dune flanks would be expected to do) rather than widening (as interdunes would). Our analysis of these interesting features is ongoing, but a combination of additional stereo observations, Earth analog studies, and modelling may be required to resolve the mystery.

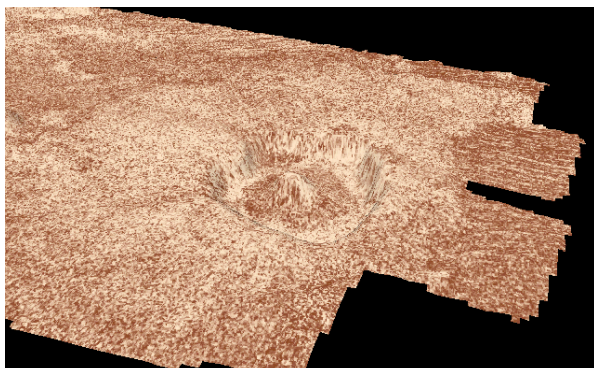


Figure 1. Perspective view of Ksa crater (D=30 km) from NW with 10x exaggeration, based on T17-T77 DTM. Note central peak, variable rim height and incursion of dunes into a low area in the ejecta blanket at right. Color is arbitrary.

T17-T77—A fresh impact crater: The T77 image, obtained in June 2011, overlaps the T17 swath and provides

strong, opposite-side stereo coverage of the 30-km diameter crater Ksa. This is one of the freshest-appearing craters on Titan and the first to be mapped in stereo. Our DTM (Fig. 1) confirms the ~750 m depth estimated from SARTopo [15], which also makes Ksa the deepest crater yet observed on Titan. The DTM also shows that elevations on the rim vary by as much as 350 m (pointing to considerable uncertainty in local measurements of crater floor-to-rim depth from SARTopo) and shows that the bright central spot in the crater is in fact a central peak that reaches nearly to the elevation of the preexisting surface. This observation thus contributes to a growing body of morphometric data that is starting to yield conclusions about the processes by which Titan craters are modified [15].

Work in Progress:

T64—Ligeia Mare redux: The T64 SAR swath, obtained in January 2010, follows the same track across the large northern seas as T25, T28, and T29, but views the terrain from the opposite side, providing much stronger stereo convergence than was previously available and potentially reducing DTM uncertainties on the subdued northern coast of Ligeia Mare from ~300 m to ~50 m and thus providing new constraints on the coastal processes at work there [16]. Ligeia Mare is the target of the Titan Mare Explorer (TiME) Discovery mission [17] now in Phase A study, which could provide ground truth about the bathymetry and possibly the shoreline topography of this area in 2023.

Collection of a DTM from these images will be challenging because the opposite illumination will reverse the contrast on slopes in hummocky terrain around the mare, and because the T64 image contains numerous gaps as a result of atmospheric interference (the infamous “rain in Spain”) when the data were downlinked, but the value of the data justifies additional effort.

Controlling and mapping the southern hemisphere: All but two of the SAR swaths obtained between T36 and T71 inclusive were located in the southern hemisphere. In particular, two sets of roughly parallel image strips cross in the south polar area, offering the prospect of a robust control network like that in the north polar zone [5]. We are in the process of constructing such a network, drawing on the image-to-image tiepoint measurements already made in support of Titan rotational modelling (i.e., the continuation of [11]). To simplify the use of the SARTopo profiles, which contain a large number of nearly redundant points but also substantial gaps, for ground control, we are gridding these observations to a uniform density and using only the data with highest confidence estimates as a control source. Once the multi-image control solution is completed, we will be able to collect on the order of 20 DTM segments, adding greatly to our knowledge of southern hemisphere topography.

References: [1] Kirk, R.L. et al. (2007) *LPS XXXVIII*, 1427. [2] Kirk, R.L. et al. (2008) *LPS XXXIX*, 2320. [3] Kirk, R.L. et al. (2009) *LPS XL*, 1413. [4] Kirk, R.L. et al. (2010) *Eos Trans. AGU*, 91(52), P22A-03. [5] Kirk, R.L. et al. (2010) Radargrammetric Mapping of Titan with Multi-Image Bundle Adjustment, *ISPRS TC IV/Autocarto/ASPRS/CaGIS Conference*, Orlando, FL, 15-19 November 2010. [6] Kirk, R.L. et al. (2012) *Icarus*, in revision. [7] Elachi, C. et al. (2004) *Space Sci. Rev.*, 115, 71. [8] Stiles, B.W. et al., (2009) *Icarus*, 202, 584. [9] Miller, S.B., and A.S. Walker (1993) *ACSM/ASPRS Ann. Conv.*, 3, 256; (1995) *Z. Phot. Fern.* 63, 4. [10] Eliason, E. (1997) *LPS XXVIII*, 331; Gaddis, L.R. et al. (1997) *LPS XXVIII*, 387; Torson, J., and K. Becker, (1997) *LPS XXVIII*, 1443. [11] Stiles, B.W. et al. (2008) *Ast. J.*, 135, 1669. [12] Radebaugh, J. et al. (2008) *Icarus*, 184, 690. [13] Neish, C.D. et al. (2010) *Icarus*, 208, 385. [14] Radebaugh, J. et al. (2012) this conference. [15] Neish, C.D. et al. (2012) this conference. [16] Stofan, E.R. et al. (2012) this conference. [17] Stofan, E.R. et al. (2011) *EPSC*, 6, EPSC2011-909.